Rotigaptide Revisited: New Insights into the Molecular Mechanisms of Gap Junction Agonism

Xianming Lin
NYU Grossman School of Medicine
Paul D. Lampe
Fred Hutchinson Cancer Center
Richard D. Veenstra
veenstrr@upstate.edu

SUNY Upstate Medical University

Systematic Review

Keywords: aap10, rotigaptide, connexin43, gap junctions, phosphorylation

Posted Date: October 17th, 2025

DOI: https://doi.org/10.21203/rs.3.rs-7715916/v1

Additional Declarations: No competing interests reported.

Title:

Rotigaptide Revisited: New Insights into the Molecular Mechanisms of Gap Junction Agonism.

Authors

Xianming Lin[1], Paul D. Lampe[2], and Richard D. Veenstra[3*]

1. Department of Medicine, NYU Grossman School of Medicine, 550 First Avenue, New York, New York 10016, Xianming.Lin@nyulangone.org
2. Translational Research Program, Public Health Sciences, Fred Hutchinson Cancer Center, 1100 Fairview Avenue North, Seattle, WA 98109-1024, USA, plampe@fredhutch.org
3. Department of Pharmacology, SUNY Upstate Medical University, 750 East Adams Street, Syracuse, New York, 13210, Veenstrr@upstate.edu

* Corresponding Author: Richard Veenstra, Ph.D., Department of Pharmacology, SUNY Upstate Medical University, 750 East Adams Street, Syracuse, New York 13210.
Email: veenstrr@upstate.edu; Phone: 315-464-5145

Abstract

It's been decades since the synthetic version of an atrial anti-arrhythmic peptide AAP10 and its D-isomer rotigaptide were developed and demonstrated to increase myocardial gap junction conductance (g_j). This increase in cardiomyocyte electrical communication was linked to PKC activation by ELISA assays, PKC activation by phorbol esters, or attenuation by biochemical inhibitors of PKCα. Studies in connexin43, -45, or -40 transfected cell lines further demonstrated that the effects of these gap junction agonists on cardiac g_j were predominantly due to gating effects on Cx43, with some on Cx45, and little or no effect on Cx40 gap junctions. Since Cx43 is known to be regulated by phosphorylation and ^{32}P was demonstrated to be incorporated into Cx43 by AAP10, the prevailing hypothesis has been that these gap junction agonists alter the gating of Cx43 gap junctions by PKC-dependent phosphorylation mechanisms. However, there are conflicting reports of PKC-downregulation of Cx43 gap junction communication and the carboxyl tail domain of Cx43 is known to contain at least 19 phosphorylation sites associated with no less than six different protein kinases. Preliminary studies in primary neonatal mouse ventricular myocyte (NMVM) cultures demonstrate that PKA and JNK inhibition prevents the acute increase in gap junction conductance (g_j) in NMVM cell pairs. JNK inhibition or 100 nM rotigaptide treatment both attenuated the 90% decline in NMVM g_j observed during perfusion with 10% normal glucose (0.1 g/L) saline solution. Together, these new preliminary observations suggest the involvement of a PKA-dependent JNK inhibitory signaling pathway in the enhancement of cardiac g_j by rotigaptide.

Keywords: aap10, rotigaptide, connexin43, gap junctions, phosphorylation

Introduction

It's been more than a quarter of a century since the discovery of an atrial anti-arrhythmic peptide and the subsequent synthesis of the synthetic peptide analog AAP10 (Gly-Ala-Gly-4Hyp-Pro-Tyr-$CONH_2$) (Aonuma, et al. 1982; Dhein, et al, 1994). First thought to have no direct cardiac membrane electrophysiological effects, AAP10 was the first therapeutic agent demonstrated to increase cardiac gap junctional coupling (Argentieri, et al. 1989; Müller, et al. 1997). These initial discoveries led to the development of additional synthetic peptides designed to increase myocardial intercellular communication via gap junction channel agonism (Dhein, et al. 2010). Rotigaptide (ZP123, Ac-D-Tyr-D-Pro-D-Hyp-Gly-D-Ala-Gly-NH_2), the most studied synthetic anti-arrhythmic peptide, is known to preserve myocardial conduction velocity during metabolic stress by acting as a gap junction agonist (Haugen, et al. 2005; Kjølbye, et al. 2003; Lin, et al. 2008; Müller, et al. 1997; Xing, et al. 2003). While there is direct evidence for the ability of rotigaptide to preserve myocardial gap junction coupling and prevent reentrant ventricular arrhythmias by increasing or preserving gap junction conductance (g_j), questions remain about the molecular and cellular mechanisms for this response. The most prominent hypothesis is that AAP10 and rotigaptide exert their effects on cardiac gap junction communication by activation of protein kinase Calpha (PKCα) and subsequent phosphorylation of connexin 43 (Cx43), the predominant connexin in mammalian cardiac ventricular gap junctions (Changri, et al. 2025; Dhein, et al. 2001, 2003; Ni, et al. 2015; Weng, et al. 2002). The functional expression of Cx43 gap junctions is known to be modulated by phosphorylation and there is a broad consensus that AAP10 and rotigaptide alter the phosphorylation state of Cx43, though the exact protein kinases and/or phosphatases involved are not entirely understood (Axelsen, et al. 2006; Solan and Lampe 2014).

The purpose of this manuscript is to review the modulation of Cx43 gap junctions by AAP10 and rotigaptide in the context of the published evidence for the PKCα modulation of cardiac gap junction conductance (g_j) and present new evidence for the involvement of other protein kinases in the regulation of cardiac ventricular gap junction g_j by rotigaptide. The new experimental evidence is based on previously published results from this laboratory on the action of rotigaptide in cardiac gap junctions between isolated pairs of neonatal mouse ventricular myocytes (NMVM, Lin, et al. 2008). Our previous study focused on the effects of continuous exposure to 0-350 nM rotigaptide for >24 hrs on the transjunctional voltage (V_j) gating of g_j in NMVM pairs. Our results confirmed an enhancement of cardiac g_j with an optimal concentration of 100 nM rotigaptide and a slowing of the V_j-dependent inactivation kinetics of g_j. Our new preliminary results focus on the acute response of NMVM g_j to 100 nM rotigaptide and the ability of rotigaptide to antagonize the decline in cardiac g_j observed during perfusion with 10% normal glucose

saline. We used a 10% normal glucose (0.1 g/L) saline solution to induce acute metabolic stress to mimic the experimental conditions utilized in the study published by Haugan et al (2005). Biochemical non-selective or selective serine/threonine protein kinase inhibition were also used to explore the roles of various serine/threonine (S/T) protein kinases in the modulation of cardiac g_j by rotigaptide.

Materials and Methods

Cardiomyocyte Dissociation. Breeding colonies of wild-type C57BL/6 (WT) and homozygous Cx40 knockout (HM Cx40 KO) mice were maintained in the SUNY Upstate Medical University Department of Laboratory Animal Resources (DLAR) vivarium. Genotype analysis was performed on all neonatal mice using the Qiagen DNeasy tissue kit (Cat. # 69506) by PCR analysis using published primer sequences for the HM Cx40KO mice (Simon, et al. 1998). Neonatal mouse hearts were dissociated, and ventricular cardiomyocytes were cultured using previously described procedures (Lin, et al. 2005, 2008). Briefly, each litter of newborn mice was anesthetized with isoflurane, sacrificed by decapitation, and their hearts removed using sterile procedures according to protocols approved by the SUNY Upstate Medical University Institutional Animal Care and Use Committee (IACUC). The ventricular cardiomyocytes were cultured in 35 mm dishes for electrophysiological examination 24-72 hrs. later.

Measurement of Gap Junction Conductance. Gap junctional current (I_j) recordings were acquired using previously established dual whole-cell patch clamp procedures with a pair of Axopatch 200B patch clamp amplifiers (Molecular Devices, LLC, San Jose, CA; Veenstra, 2001; Wei, et al. 2019). Whole-cell input capacitance (C_{input}) was measured using a +5 mV, 10 ms voltage step applied to both cells of a NMVM cell pair from a holding potential of −40 mV. Whole-cell patch electrode (access) resistances (R_{el1} and R_{el2}) were calculated using the equation $R_{el} = \tau_{cap}/C_{input}$, where τ_{cap} is the single-cell capacitive current decay time constant. The macroscopic junctional conductance (g_j) was calculated using the equation: $g_j = -\Delta I_2/[(V_1 + \Delta V) - V_2]$, where I_1 and I_2 are whole-cell currents, V_1 and V_2 are command (holding) voltages, (ΔV) is a voltage step applied to one cell while maintaining the holding potential (V_h) of the partner cell, ΔI_2 is the change in whole-cell current of the partner cell, and (V1 + ΔV) − V2 is the transjunctional potential, V_j. For all g_j experiments, V_h = 0 mV for both cells, ΔV was a 5 s, −20 mV pulse applied four times/min, and g_j was normalized by dividing the time-dependent g_j by the initial g_j measurement, or $G_j = g_j(time)/g_j(initial)$. For all perfusion experiments, g_j(initial) was calculated as the g_j averaged over the first 2 min preceding perfusion (8 data points). To more accurately calculate g_j, the whole-cell patch

electrode resistances, R_{el1} and R_{el2}, were subtracted from the $g_j = -\Delta I_2/V_j$ calculation where the actual g_j = apparent g_j – $(1/R_{el1} + 1/R_{el2})$, i.e. the observed r_j = actual $r_j + R_{el1} + R_{el2}$).

Bath Perfusion. Bath perfusion was performed by gravity-fed lines and mini-pump extraction of an equivalent bath volume (1 ml/min, 3 ml bath volume). Solution exposure was essentially instantaneous and laminar to avoid disruption of the ongoing DWCR procedures. Continuous solution extraction occurred at the opposite outer edge of the 35 mm culture dish. Tetrodotoxin (30 μM TTX, Sigma) was added to the bath saline (mM: NaCl 142, KCl 1.3; CsCl 4, TEACl 2, $MgSO_4$ 0.8, NaH_2PO_4 0.9, $CaCl_2$ 1.8, dextrose 5.5 (=1 g/L), HEPES 10, pH 7.4 with 1 N NaOH) of each dish to prevent sodium current activation during the DWCR experiments. The low glucose saline is identical in composition except for the addition of only 0.1 g/L L-glucose, 10% of normal. Patch pipettes were filled with a KCl internal pipette solution (IPS KCl, in mM: KCl, 140; $MgCl_2$, 1.0; $CaCl_2$, 3.0; BAPTA, 5.0; HEPES, 25; pH titrated to 7.4 using 1N KOH; ≈ 200-300 nM free [Ca^{++}]). The final osmolarity of both external and internal solutions was adjusted to 310 mosm by dilution with 18 MΩ-cm deionized water or salt addition as required by determination using a freezing point osmometer (Advanced Instruments Model 3W2). All perfusion lines were rinsed with 70% ethanol and deionized water after daily use.

Pharmacological treatments. Rotigaptide was provided to RDV in powder form by Wyeth Research and stored desiccated at -80 °C. A 100 μM weekly stock solution of rotigaptide was prepared and diluted to the optimal concentration of 100 nM based on our previous study (Lin, et al. 2008). Stock solutions were diluted daily as needed in saline for short-term and M199 media for long–term (e.g. overnight) treatments.
S/T protein kinase inhibition. All S/T protein kinase inhibitors were purchased from Calbiochem and the experimental concentrations were determined based on the inhibitory profiles provided in the Calbiochem Inhibitor SourceBook (2nd Ed.).
H-7: K_I = 3.0 μM for PKA; 6 μM for PKC; 5.8 μM for PKG, and 97 μM for MLCK);
H-89: 48 nM = K_I for PKA, K_I = 270 nM, RhoKII; ≥ 30 μM for CaMKII, CK1, PKC, and MLCK;
bisindolylmaleimide I (BIM): PKC IC_{50} (nM) ≅ 8 (α), 18 (βI), 210 (δ), 132 (ε), 5800 (ζ);
JNK inhibitor II: IC_{50} = 40 nM for JNK1/2 (MAPK8/9), 90 nM for JNK3 (MAPK10);
JNK inhibitor I peptide: IC_{50} ≅ 1 μM; PKA inhibitor peptide 6-22 amide: K_I = 1.7 nM.
Protein phosphatase inhibition: Okadaic acid; K_I = 100 pM for PP2A; 10-15 nM for PP1, 5 μM for PP2B.

Phospho-Cx43 immunoblot analysis. Matched control or 10% normal glucose saline and 100 nM rotigaptide treated 60 mm ventricular culture dishes were prepared and cell samples collected in ice cold PBS + Roche mini-EDTA-free protease inhibitors + 1 mM PMSF, frozen, stored at -80 °C, and immunoblotted for Cx43 phosphoserine analysis using

phospho-specific Cx43 antibodies developed by Dr. Paul Lampe at the Fred Hutchinson Cancer Center in Seattle, WA. In these preliminary studies, the Cx43 phosphorylation state of S262, S279, and S365 were examined in Dr. Lampe's laboratory using NMVM cultures after 10 min exposure to normal bath saline, normal saline plus 100 nM rotigaptide (acute exposure), 10% normal glucose saline, and 10% normal glucose saline ±100 nM rotigaptide pretreatment (overnight + bath saline) (Lampe, et al. 1998; Solan, et al. 2007; Warn-Cramer, et al. 1996).

Results

The results presented herein are preliminary results from the continuation of a research project initiated in my laboratory in collaboration with Paul Lampe and the cardiovascular division of Wyeth Pharmaceutical (Philadelphia, PA) and Zealand Pharma (Soborg, Denmark) prior to Wyeth's merger with Pfizer in 2009 and the subsequent shutdown of their cardiovascular research division. The intent of this manuscript is to present data and potential new insights into the signaling mechanisms involved in the agonism of cardiac gap junctions by rotigaptide in the context of the existing published literature rather than make formal conclusions as to the molecular mechanisms involved in the functional upregulation of Cx43 gap junction communication.

Acute perfusion of NMVM cell pairs with 100 nM rotigaptide produced a 5.6% increase in G_j relative to the initial g_j measured during a 2-minute control period (Figure 1A, ●, n = 3). Control perfusions with normal saline in untreated NMVM cell pairs did not produce any change in G_j (■, n=4). Similar experiments performed on NMVM cell pairs isolated from homozygous connexin40 knockout mice (HM Cx40) hearts produced a 12.8% increase in G_j when perfused with 100 nM rotigaptide (▲, n-3). These results indicate that rotigaptide can open existing Cx43 cardiac gap junction channels and that the trace amounts of Cx40 expressed in ventricular myocytes may impede the rotigaptide response, perhaps by steric hindrance.

PKCα is proposed to be responsible for the functional upregulation of cardiac gap junction conductance induced by AAP10 and rotigaptide (reviewed in Dhein, et al. 2010). To investigate the role of serine/threonine (S/T) protein kinases in the rotigaptide response, NMVM cultures were preincubated overnight with chemical S/T protein kinase inhibitors (Figure 1B) and perfused with 100 nM rotigaptide the next day in the continued presence of the inhibitor. Non-specific S/T kinase inhibition with 12 μM H-7 abolished the acute response to 100 nM rotigaptide perfusion (◆, n=3). However, pretreatment with 100 nM H-89, a concentration that should be selective for protein kinase A (PKA) inhibition relative to

PKC and other S/T protein kinases, also blocked the acute g_j response to 100 nM rotigaptide perfusion in NMVM cell pairs (▼, n=3).

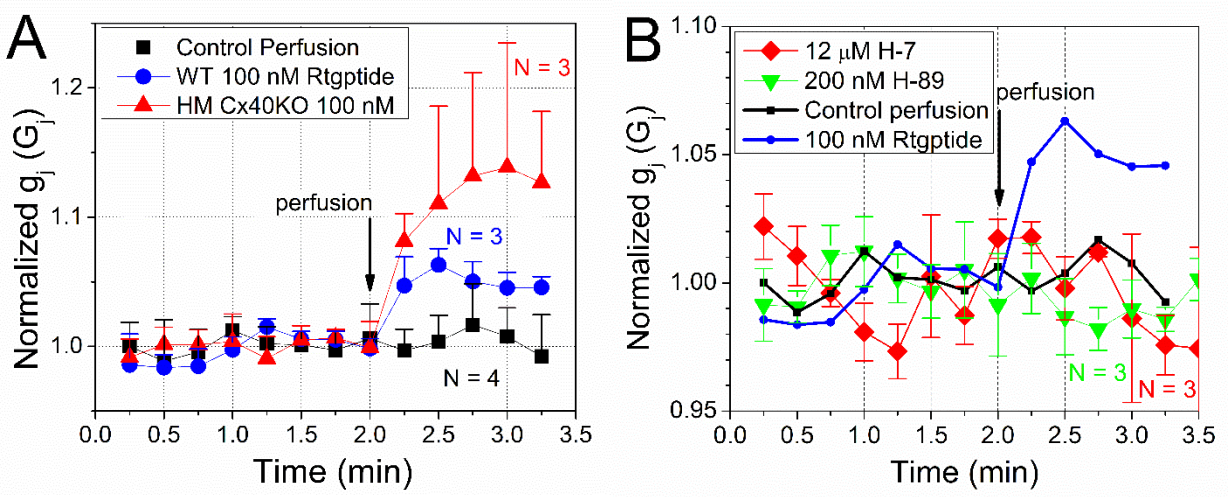

Figure 1 Acute perfusion with rotigaptide. (**A**) Perfusion of neonatal mouse ventricular cardiomyocyte (NMVM) cell pairs isolated from wild-type (●) and homozygous connexin40 (HM Cx40 KO, ▲) hearts with 100 nM rotigaptide produced an ≈6% and ≈13% in gap junction conductance, respectively. Control perfusion with normal saline (■) had no effect on cardiac g_j measured during 5 sec duration, -20 mV transjunctional voltage (V_j) pulses applied 4 times per minute and normalized (G_j) to the average g_j value obtained during the first 2 min of each experiment. Only NMVM cell pairs with stable baseline G_j values were used for experimental purposes. (**B**) Non-selective serine/threonine (S/T) protein kinase inhibition with 12 μM H-7 (◆) or selective protein kinase A (PKA) inhibition with 200 nM H-89 (▼) both blocked the response to 100 nM rotigaptide perfusion.

To examine the effect of PKC inhibition on the acute rotigaptide response, NMVM cell cultures were pre-incubated with 200 or 500 nM bisindolylmaleimide (BIM) and perfused with 100 nM rotigaptide (Figure 2A). PKC inhibition by 200 nM BIM, which is relatively selective for PKC isoforms α, β1, δ, and ε, failed to inhibit the acute rotigaptide response, though there was a slight delay in the increase in G_j (▼, n=2). One experiment performed with 500 nM BIM effectively prevented the acute increase in G_j upon 100 nM rotigaptide perfusion (◆). To further our examination of S/T protein kinase inhibition on the acute effect of rotigaptide, we applied 200 nM c-Jun N-terminal kinase (JNK)1/2/3 inhibitor overnight and performed perfusion experiments on NMVM cell pairs as before (Figure 2B). In all three experiments, JNK inhibitor II effectively prevented the acute increase in G_j induced by 100 nM rotigaptide exposure (▲). Taken together, these preliminary results indicate a greater involvement of PKA and JNK S/T protein kinases in the agonism of cardiac ventricular G_j than PKC isoforms.

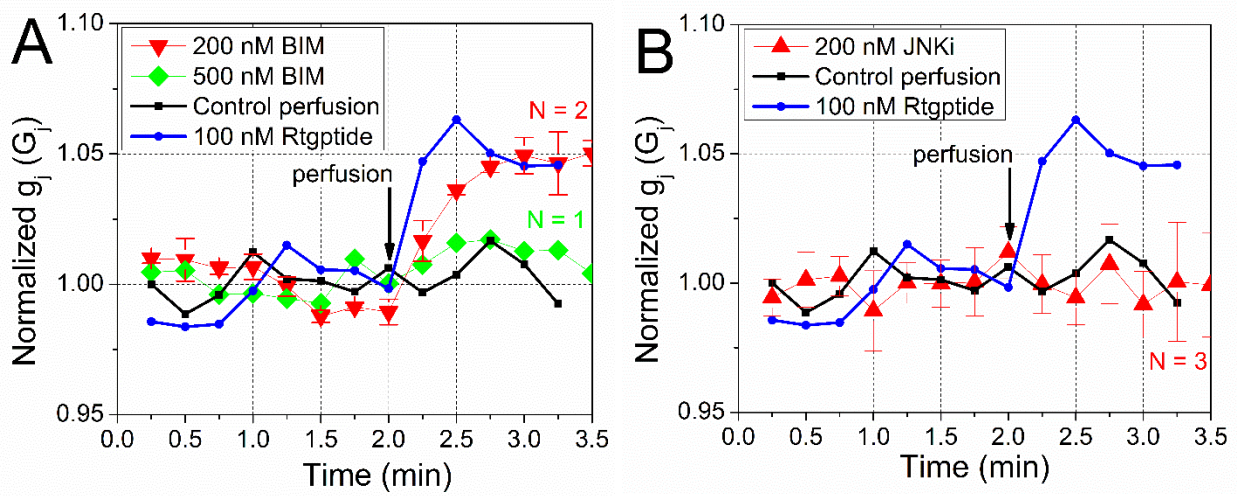

Figure 2 Inhibition by protein kinase C (PKC) and Janus N-terminal kinase (JNK). (**A**) The increase in G_j induced by 100 nM rotigaptide perfusion was at most delayed slightly by treatment of NMVM cultures with 200 nM bisindolylmaleimide (BIM) to inhibit the α-, β-, δ-, and ε- forms of PKC (▼) but was inhibited by 500 nM BIM (◆). (**B**) Pretreatment with 200 nM JNK II inhibitor (JNKi, ▲) prevented the acute increase in G_j observed during 100 nM rotigaptide perfusion, suggesting the involvement of JNK in the regulation of cardiac g_j.

One disadvantage of chemical S/T protein kinase inhibitors is that their selective inhibitory effects are concentration-dependent, i.e., they are relatively selective among the various forms of S/T protein kinases. Thus, we decided to use specific kinase-derived peptide inhibitors to improve the selective effects of PKA and JNK inhibition on the acute rotigaptide response. Addition of 5 nM PKA Inhibitor 6-22 amide (PKAi peptide) to the internal pipette solution of the whole cell patch pipettes prevented the acute rotigaptide response in two NMVM cell pairs (Figure 3A, ▼, n = 2). Although the JNK inhibitor I (JNKi) peptide is cell-permeable, we found this peptide inhibitor to be more effective by adding it to the pipette solution as was performed with the PKAi peptide. In three experiments, 2 μM JNKi peptide also prevented the acute increase in G_j induced by rotigaptide perfusion of NMVM cell pairs (Figure 3B, ▲). In these preliminary experiments, the negative control JNKi peptide was not tested. These inhibitory protein kinase peptide experiments suggest greater involvement of PKA and JNK S/T protein kinases in the gap junction agonist response to rotigaptide treatment than the prevailing PKCα hypothesis.

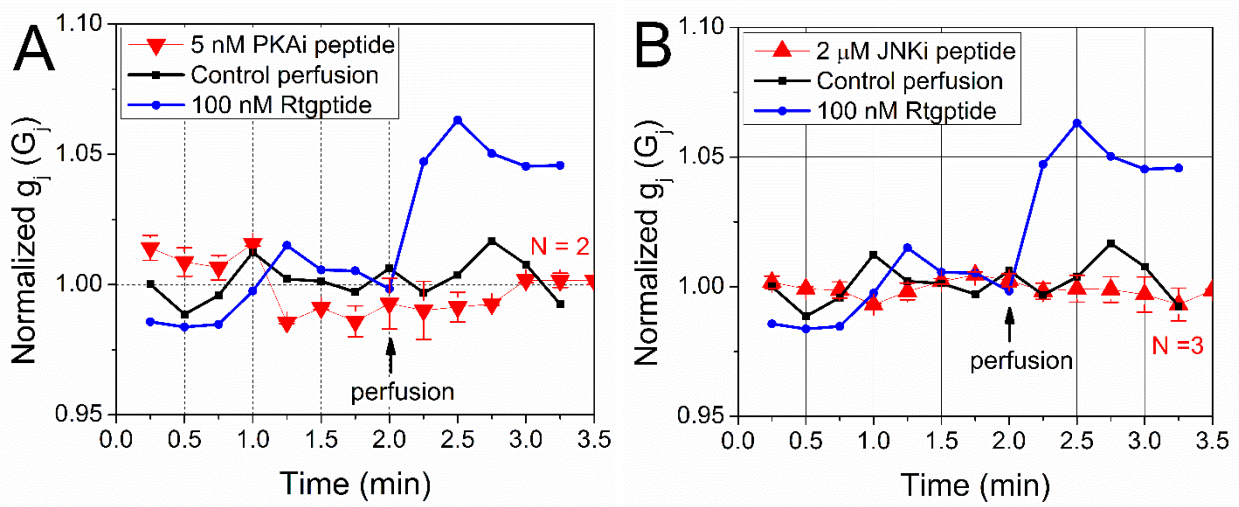

Figure 3 PKA and JNK inhibitory peptide inhibition of the acute rotigaptide response. (**A**) Selective PKA inhibition by inclusion of 5 nM PKA inhibitor 6-22 amide (PKAi peptide, ▼) in the whole cell recording patch pipettes blocked the 100 nM rotigaptide induced increase in G_j. (**B**) Similarly, addition of 2 μM of the JNK inhibitory peptide (▲) to the recording patch pipettes prevented the acute rotigaptide response in NMVM cell pairs. These selective intracellular peptide inhibitor experiments implicate PKA and JNK in the modulation of cardiac g_j and the response to rotigaptide.

The beneficial effects of rotigaptide are based primarily on the ability to improve myocardial gap junction communication during myocardial ischemia or metabolic stress which, in turn, preserves conduction velocity, reduces action potential dispersion, and possibly reduces infarct size, all of which can suppress myocardial arrhythmogenic activity (Dhein, et al. 2003; Haugen, et al. 2005, 2006; Hennan, et al. 2006; Kjølbye, et al. 2008; Shiroshita-Takeshita, et al. 2007; Takemoto, et al. 2012; Xing, et al. 2003). To mimic metabolic stress on our NMVM preparations, we experimented with low glucose saline perfusion. Bath perfusion (1 ml/min, ≈3 ml bath volume) with zero-glucose saline produced complete g_j uncoupling and cell death within minutes that could not be rescued with normal saline perfusion. Activation of a large outward current, presumably the K_{ATP} channel current, was observed just prior to cell death and loss of the whole cell recordings (data not shown). Perfusion with 25% normal glucose (0.25 g/L) saline consistently reduced g_j by about 50% (N = 3) whereas 10% normal glucose saline perfusion produced a ≥90% steady state reduction in G_j within 10 min. Thus, we chose 10% normal glucose saline to test the effects of rotigaptide and S/T protein kinase inhibition on G_j between paired NMVMs.

Figure 4A illustrates the time course of g_j uncoupling induced by 10% normal glucose saline perfusion in NMVM cell pairs. Exposure to 10% normal glucose saline steadily reduced g_j by

> 95% within 10 min in NMVM cell pairs (n=4, ■). NMVM cell cultures pretreated and bathed with 100 nM rotigaptide during the 10% normal glucose perfusion experiments limited the decline in G_j during the first 10 min of low glucose perfusion to 40% and the maximum reduction in G_j over the 25 min course of two experiments was limited to ≈75% (n=2, ●). These results are consistent with the ability of rotigaptide to reduce myocardial uncoupling during conditions of metabolic stress (Haugen, et al. 2005; Xing, et al. 2003). To explore the involvement of S/T protein kinases on the action of rotigaptide, the JNK inhibitor II (JNKi) experiment was repeated by pretreating and bathing NMVM cell cultures with 200 nM JNK inhibitor II (JNKi) and perfusing with 10% normal glucose saline (Figure 4B). In two experiments, the decline in G_j was slowed but still achieved 90% uncoupling within 15 minutes of low glucose perfusion (▲). Since only a partial response was achieved with the 200 nM JNKi, 100 nM rotigaptide was included in the bath solution along with 200 nM JNKi and NMVM cell pairs were perfused with 10% normal glucose saline (▼, n=2). The combination of rotigaptide + JNKi closely matched, but did not exceed, the response achieved with 100 nM rotigaptide treatment and 10% normal glucose saline perfusion. The effect of 2 mM JNKi peptide on the 10% normal glucose saline induced decline in G_j was examined in two NMVM cell pairs (◆, n=2). Inclusion of the JNKi peptide in the whole cell patch pipettes blocked the G_j decline as well as 100 nM rotigaptide alone or in combination with the JNK II inhibitor, indicative of a predominant role of JNK in the low glucose uncoupling response.

Since the central hypothesis is that rotigaptide increases myocardial g_j by modulating phosphorylation of Cx43, it follows that S/T protein phosphatases may also affect the g_j uncoupling induced by low glucose in NMVM cells. To examine the effect of S/T protein phosphatase inhibition on the uncoupling induced by 10% normal glucose saline perfusion, NMVM cultures were pretreated overnight with 1 or 30 nM okadaic acid to inhibit protein phosphatase 2A (PP2A, IC_{50} = 100 pM) and protein phosphatase 1 (PP1, IC_{50} = 10-15 nM) with minimal effect on protein phosphatase 2B (PP2B, IC_{50} = 5 μM). Treatment with 1 nM okadaic acid reduced the rate of the G_j decay during 10% normal glucose saline perfusion (≈70% after 10 min of perfusion), but it did not match the effect of 100 nM rotigaptide on the low glucose g_j decay (Figure 4C, n=2, ▲). Increasing the okadaic acid concentration to 30 nM to inhibit PP1 further reduced the decline in G_j induced by 10% normal glucose saline perfusion (≈50% at the 10 min perfusion timepoint, n=2, ▼), but the effect was still less than the effect of 100 nM rotigaptide. Combining 100 nM rotigaptide with 30 nM okadaic acid closely matched the 40% decline in G_j observed with 100 nM rotigaptide alone or in combination with 200 nM JNKi (n=2, ◆). These results are all consistent with the modulation of S/T phosphorylation being the primary mechanism for

the regulation of NMVM G_j by rotigaptide but are also indicative of a role of JNK and PP1/PP2A in the modulation of myocardial g_j.

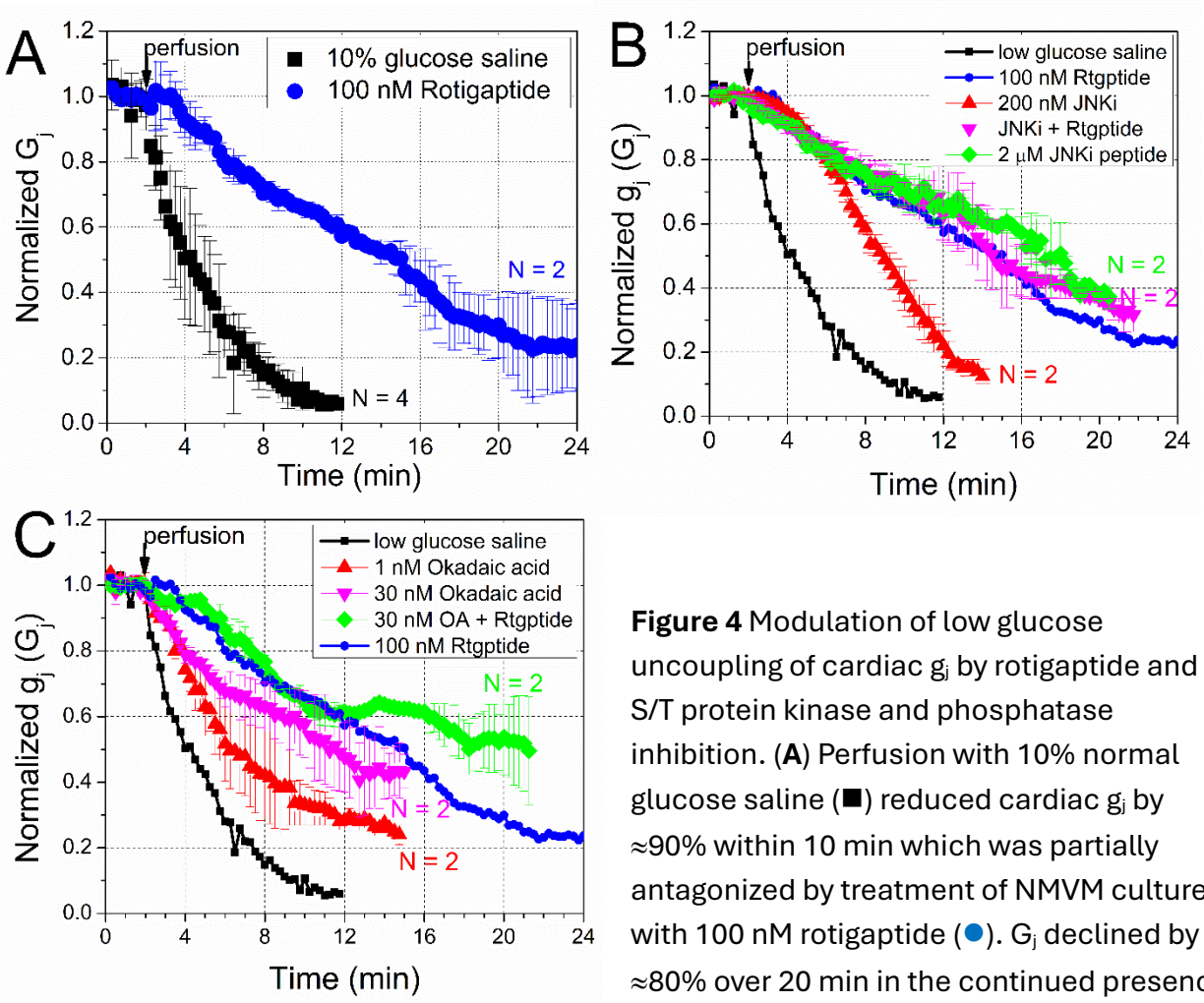

Figure 4 Modulation of low glucose uncoupling of cardiac g_j by rotigaptide and S/T protein kinase and phosphatase inhibition. (**A**) Perfusion with 10% normal glucose saline (■) reduced cardiac g_j by ≈90% within 10 min which was partially antagonized by treatment of NMVM cultures with 100 nM rotigaptide (●). G_j declined by ≈80% over 20 min in the continued presence of 100 nM rotigaptide during low glucose saline perfusion. (**B**) Treatment with 200 nM JNK inhibitor II (JNKi, ▲) slowed the low glucose induced decline in G_j but the co-application of 100 nm rotigaptide (▼) reduced the decline of G_j to that observed with rotigaptide treatment alone. However, addition of 2 μM JNK inhibitor peptide (JNKi peptide, ◆) to the recording patch pipettes prevented the low glucose-induced decline in G_j as effectively as the 100 nM rotigaptide treatment with or without the JNKi inhibitor. (**C**) The effect of S/T protein phosphatase inhibition on low glucose-induced uncoupling was also examined in NMVM cell pairs by treatment with 1 nM (▲) or 30 nM (▼) okadaic acid. Okadaic acid treatment reduced the decline in low glucose-induced G_j in a concentration-dependent manner, suggesting the involvement of both protein phosphatase 2A (PP2A) and protein phosphatase 1 (PP1). Contrary to the results with the JNKi peptide + rotigaptide, the effects of 30 nM okadaic acid plus 100 nM rotigaptide (◆) were additive as observed by the further reduction of the low glucose-induced decline in cardiac G_j

The modulation of gap junctions by phosphorylation of Cx43 has been expertly reviewed in Solan and Lampe (2014) and the alteration of some Cx43 phosphorylation sites by ischemia have also been described (Axelsen, et al. 2006). Based on a body of published literature, the prevailing hypotheses are that phosphorylation of Cx43 at sites Y247, S262, S279/282, and S368 by Src-kinase, $p34^{cdc2}$, MAPK, and PKC promote gap junction disassembly and downregulation of g_j, whereas Cx43 phosphorylation at sites S325/328/330, S373, S364, and S365 by casein kinase 1 (CK1), Akt, and possibly PKA promote gap junction assembly and g_j upregulation (Cooper and Lampe 2002; Kanemitsu, et al. 1998; Lampe, et al., 1998, 2000; Lin, et al. 2001; Park, et al. 2007; Solan, et al. 2007; Solan and Lampe, 2014; TenBroeck, et al. 2001; Warn-Cramer, et al. 1996). Particularly germane to the PKC hypothesis, phosphorylation of S365 is proposed to serve as a "gate-keeper" to prevent PKC phosphorylation of S368 and subsequent downregulation of Cx43-mediated gap junction communication (Solan, et al. 2007). Thus, in collaboration with Dr. Paul Lampe at the Fred Hutchinson Cancer Center, we examined the phosphorylation state of S262, S279, and S365 of Cx43 using phospho-specific antibodies he's developed on NMVM cultures under the experimental conditions presented in this preliminary study.

Two sets of experimental conditions were examined in NMVM cultures, control (untreated) conditions and 100 nM rotigaptide treatment (10 min), and 10% normal glucose saline exposure for 10 min in the presence or absence of 100 nM rotigaptide. Immunoblots of total Cx43 protein and phosphoserine-specific Cx43 from NMVM cultures are shown in Figure 5. Rotigaptide treatment (100 nM, 10 min) appeared to increase pS365 content and decrease pS262 and pS279 content, consistent with an upregulatory response of Cx43-mediated gap junction communication (lanes 1 and 2). Conversely, bath exposure to 10% normal glucose saline for 10 minutes appeared to reduce Cx43 pS365 content while increasing pS262 and pS279 content (lane 3), consistent with downregulation of Cx43 g_j. However, 100 nM rotigaptide treatment (overnight plus 10 min bath) apparently reduced the pS262 and pS279 content and lessened the reduction in pS365 content under low glucose conditions (lane 4), again consistent with the ability of rotigaptide to reduce the downregulation of Cx43-mediated gap junction communication during conditions of metabolic inhibition.

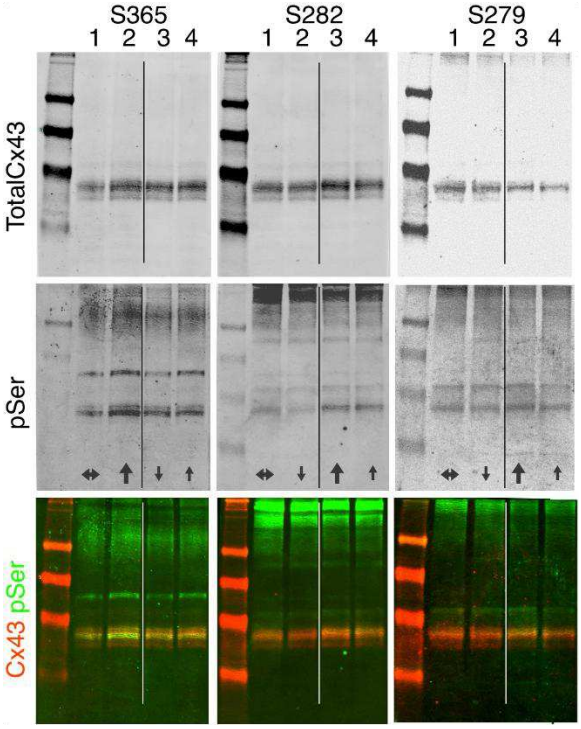

Figure 5 Cx43 total protein and phosphoserine-specific immunoblots from WT NMVM cultures. The top panels are the total Cx43 protein immunoblots for S365, S262, and S279 for the corresponding phospho-serine specific (pSer, middle panels) immunoblots and fluorescent images (lower panels) of the total Cx43 (Cx43) and phospho-serine (pSer) immunoblots under different experimental conditions. Lane 1 is the Cx43 immunoblot analysis of one 60 mM NMVM culture dish after 10 min in control saline and lane 2 is another NMVM culture dish from the same dissociation after 10 min treatment with 100 nM rotigaptide. Lane 3 represents a similar experiment where an NMVM culture dish was exposed to 10% normal glucose saline for 10 min and another NMVM culture dish was pretreated with 100 nM rotigaptide (overnight) prior to and during the exposure to 10% normal glucose saline. The arrows indicate relative increase or decrease in Cx43 phosphoserine content relative to the control conditions (lane 1, ↔) under their respective experimental conditions. Lanes 1&2 and 3&4 were from the same primary myocyte cultures. 100 nM rotigaptide (lane 2) increased (↑) Cx43 pS365 and reduced (↓) pS262 and pS279 content relative to control NMVM culture conditions. Acute exposure to 10% normal glucose saline (lane 3) had the opposite effect of reducing pS365 and increasing pS262 and pS279 content but these changes were partially ameliorated by 100 nM rotigaptide pretreatment (overnight, lane 4).

Discussion

There is substantial evidence that AAP10 and its synthetic D-isomer, rotigaptide, increase cardiac gap junction g_j under normal or conditions of metabolic stress like ischemia (Haugen, et al. 2005; Kjølbye, et al. 2003; Lin, et al. 2008; Müller, et al. 1997; Xing, et al. 2003). Despite a lack of effects on action potential duration (APD) or refractoriness, these synthetic anti-arrhythmic peptides can reduce APD dispersion, preserve or prevent declines in myocardial conduction velocity during episodes of metabolic stress, and may limit the development of reentrant ventricular tachycardias and atrial fibrillation during periods of ischemia (Dhein, et al. 2003; Haugen, et al. 2005, 2006; Hennan, et al. 2006; Kjølbye, et al. 2008; Shiroshita-Takeshita, et al. 2007; Takemoto, et al. 2012; Xing, et al. 2003). The ability of rotigaptide to reduce infarct size after ischemia/reperfusion injury are mixed, with some studies reporting reduced infarct size (Haugan, et al. 2006; Hennan, et al. 2006), or none at all (Xing, et al. 2003). These therapeutic effects are largely attributed to the agonist actions of rotigaptide on existing cardiac gap junctions, i.e. gating, though increases in Cx43 expression with longer term treatments have also been noted (Stahlhut, et al. 2006). Ventricular gap junctions are composed predominantly of Cx43 while Cx40 is also abundantly expressed in the atria and ventricular conduction system (Davis, et al. 1995). However, rotigaptide appears to modulate Cx43 gap junctions with negligible effects on Cx40 or non-myocardial connexin gap junctions composed of Cx26 and Cx32 (Clarke, et al. 2006; Hagen, et al. 2009). Our preliminary results in NMVM gap junctions are consistent with this apparent connexin-specificity of rotigaptide for Cx43 gap junctions since the g_j increase in response to 100 nM rotigaptide was enhanced by the knockout of Cx40 in NMVMs (Fig. 1A).

The hypothesis that AAP10 and rotigaptide increase cardiac g_j by activation of PKC is based primarily on evidence of PKC activation, measured by ELISA assays, in cardiomyocytes or Hela-Cx43 cells, and the observed increase in g_j which could be inhibited by PKC inhibitors, e.g. BIM, HBDDE, or CGP 43545, all of which inhibit PKCα (Dhein, et al. 2001, 2003; Weng, et al. 2002). Our preliminary results in NMVMs with PKC inhibition by BIM illustrate that the acute increase in G_j upon 100 nM rotigaptide perfusion was inhibited only by higher concentrations of BIM that would inhibit multiple isoforms of PKC (Fig. 2A). Conversely, PKA and JNK inhibition by bath applied chemical (H-89, JNK inhibitor II) or intracellular selective peptide (PKA inhibitor peptide 6-22 amide, JNK inhibitor I peptide) inhibitors abolished the acute rotigaptide response (Figs. 1B, 2B, 3A&B). Thus, our preliminary results from NMVM cell pairs indicate that PKA and JNK are also involved in the control response to rotigaptide.

How AAP10 and rotigaptide activate protein kinases in cardiomyocytes remains somewhat of a mystery. Radioligand binding studies with ^{14}C-AAP10 indicated a saturable cardiac membrane binding site with a K_d of 0.88 nM that exhibited competitive binding with the natural AAP10 (Gly-Pro-4Hyp-Gly-Ala-Gly, AAPnat) peptide (Anouma, et al. 1982; Weng, et al., 2002). Attempts to isolate, purify, and identify the apparent 200kDa membrane receptor were unsuccessful due to low yields. However, the non-hydrolysable GDP analog, GDP-βS was able to inhibit AAP10-dependent ^{32}P incorporation into Cx43 in HeLa-x43 cells, indicative of a G-protein coupled receptor (GPCR) as the AAP10 membrane binding site (Weng, et al. 2002). A competitive binding assay with rotigaptide and radiolabeled ligands for 80 known GPCRs and ion channels did not demonstrate any high affinity binding to any of the known membrane receptors or channels (Haugan, et al. 2005). Thus, the molecular identity of the presumed GPCR for AAP10 and/or rotigaptide remains unknown.

The ability to improve myocardial g_j during ischemia or metabolic stress is the major tenet of the antiarrhythmic action of AAP10 and rotigaptide. Because ischemia is difficult to replicate *in vitro* (e.g. hypoxia), we chose to perfuse NMVM cultures with a 10% (0.1 gm/L) glucose saline solution to induce metabolic stress, which consistently produced a 90% decline in g_j without causing cell death during a 10 min perfusion period. Pretreatment with 100 nM rotigaptide slowed and reduced the magnitude of the low glucose-induced G_j decline in NMVM cell pairs (Fig. 4A). To the best of our knowledge, no other laboratory has used low glucose conditions to examine the agonistic effect of rotigaptide on cardiomyocyte g_j under conditions of metabolic stress. Novel observations with chemical and peptide JNK inhibitors further revealed the ability of selective JNK inhibition to mimic the effects of 100 nM rotigaptide on NMVM G_j under metabolic stress conditions (Fig. 4B). The combined effects of JNK inhibition and rotigaptide treatment were comparable, but not additive, indicative of convergent mechanisms of action. The inhibition of dephosphorylation by 1 or 30 nM okadaic acid pretreatment also progressively prevented the decline in NMVM G_j during low glucose saline perfusion, partially indicative of the involvement of Cx43 dephosphorylation events by PP2A and PP1 in the metabolic stress-induced decline in cardiac G_j (Fig. 4C). The PP2A/PP1 inhibition by 30 nM okadaic acid did not equal the G_j preserving action of 100 nM rotigaptide, and the addition of 100 nM rotigaptide further opposed the low glucose-induced decline in NMVM G_j. The combination of the two appears to further reduce the decline in G_j after > 10 min of low glucose saline perfusion, suggestive of Cx43 phosphorylation and dephosphorylation events in the regulation of cardiac g_j under conditions of metabolic stress.

The first observations of increases in cardiac electrical coupling date back to the 1980s when β-adrenergic stimulation, known to increase intracellular cAMP levels, intracellular injection of cAMP, or application of membrane-permeable analogs of cAMP (dibutyryl- and

8-bromo-cAMP) all increased gap junction conductance or permeability in mammalian cardiac tissues (Atkinson, et al. 1995; Burt and Spray, 1988; DeMello, 1986; 1989; DeMello and Van Loon, 1987). While the effects of β-adrenergic stimulation or cAMP analogs on electrical communication can be observed within minutes, Cx43 mRNA and protein levels also increase in cardiac tissues over a 4 -24 hr period (Darrow, et al., 1996). Though not linked to a specific protein kinase, these studies uniformly indicate an upregulation of g_j by cAMP-dependent mechanisms in cardiac myocytes and tissues. The PKC hypothesis for the gap junction agonism exhibited by AAP10 and rotigaptide is based on the published observations of concomitant increases in g_j and PKC activation with AAP10 and rotigaptide application to cardiomyocytes or HeLa cells expressing Cx43 (Dhein, et al. 2001, 2003; Ni, et al. 2015; Weng, et al. 2002). The basis for suggesting the involvement of the PKCα isoform is based primarily on the relative inhibitory selectivity of the PKC inhibitors used. While these initial observations are not in question, numerous other studies on the effect of PKC activation on Cx43 gap junctions have indicated a downregulation of Cx43 gap junction communication by PKC (e.g. Enomoto and Yamasaki, 1985; Kanemitsu, et al. 1993; Koo, et al. 1997; reviewed in Solan and Lampe, 2005). Two studies have revealed that PKC activation caused a reduction in the single Cx43 gap junction channel conductance from the ≈100 pS to the ≈50 pS state, consistent with observed reductions in Cx43 g_j (Lampe, et al. 2000; Ek-Vitorin, et al. 2006).

The role of Cx43 phosphorylation state in the assembly and disassembly of gap junctions has been extensively studied and excellent reviews on the subject have already been published (Ai, et al. 2021; Solan and Lampe, 2014, 2020). Early studies with Cx43 indicated that phosphorylation is required for Cx43 to assemble into gap junctions (Musil, et al. 1990), Cx43 gap junction assembly is also promoted by casein kinase 1 (CK1), cAMP-dependent PKA, and Akt (Cooper and Lampe, 2002; Dunn and Lampe, 2014; Solan, et al. 2007; TenBroek, et al. 2001). Conversely, cell cycle and growth activated kinases like $p34^{cdc2}$ and mitogen-activated protein kinases (MAPKs), PKC, and Src tyrosine kinases are associated with downregulation of gap junction communication and internalization of Cx43-containing gap junctions (Doble, et al. 2004; Hossain, et al., 1998; Kanemitsu, et al. 1998; Koo, et al. 1997; Lampe, et al. 2000; Lin, et al. 2001; Solan and Lampe, 2020; Swenson, et al., 1990; Warn-Cramer, et al. 1996). Many of the protein kinase dependent Cx43 phosphorylation sites have been identified and those reportedly involved in promoting gap junction formation include S325/328/330 (CK1; Cooper and Lampe, 2002), S373 (Akt; Dunn and Lampe, 2014), and S364/365 (PKA; Solan, et al. 2007; TenBroek, et al. 2001). The Cx43 phosphorylation sites linked to Cx43 gap junction disassembly include S255, S262, and S279/282 (MAPK and p34cdc2; Doble, et al. 2004; Kanemitsu, et al. 1998; Warn-Cramer, et al. 1996;), S368 (PKC; Hossain, et al., 1998; Koo, et al. 1997; Lampe, et al,

2000), and Y247 and Y265 (Src; Lin, et al. 2001; Solan and Lampe, 2020; Swenson, et al., 1990).

Hypoxic and ischemic conditions are known to produce myocardial electrical uncoupling and Cx43 dephosphorylation of Cx43 sites S325/328/330 and S365 (Beardslee, et al. 2000; Lampe, et al. 2006; Solan, et al., 2007). It has also been demonstrated that phosphorylation of the S365 site prevents phosphorylation of the S368 site and dephosphorylation of S365 in hypoxic hearts is reciprocally correlated with an increase in pS368 content (Lampe, et al. 2000; Solan, et al. 2007). These observations have prompted the hypothesis that pS365 serves as a "gatekeeper" to prevent S368 phosphorylation and protect against PKC-mediated down-regulation of Cx43 gap junction content and function (Solan, et al., 2007). Thus, we chose to examine the phosphorylation state of key Cx43 upregulatory and downregulatory phosphorylation sites S365 and S262 and S279 under normal and low glucose conditions in the presence and absence of 100 nM rotigaptide (Figure 5). Under normal culture conditions, 100 nM rotigaptide increased the pS365 content and reduced the pS262 and pS279 protein content, consistent with an increase in NMVM Cx43 gap junction function. Ten min exposure to 10% normal glucose saline had the opposite effect of decreasing pS365 and increasing pS262 and pS279 Cx43 content in NMVM cell cultures, consistent with the decline in G_j observed during the DWCR perfusion experiments, but pretreatment with 100 nM rotigaptide partially antagonized these downregulatory phosphorylation responses by preserving some pS365 content and reducing the increase in pS262 and pS279. These Cx43 phosphorylation responses to 100 nM rotigaptide and low glucose certainly implicate the actions of other S/T protein kinases in the pharmacological action of rotigaptide and the responses to metabolic stress.

Additional studies of the Cx43 phosphorylation regulation of cardiac gap junction communication report that: PKCepsilon (PKCε) phosphorylates Cx43 (Bowling, et al. 2001; Doble and Kardami, 2000); phorbol esters and growth factors activate protein kinases in addition to PKC (Hossain, et al. 1998, 1999; Sirnes, et al. 2009); cAMP activates both the exchange protein (Epac)- and PKA-dependent signaling pathways (Kwak, et al. 2008; Somekawa, et al. 2005); and there are at least three additional Cx43 phosphorylation sites S296, S297, and S306 that are not linked to any specific kinases yet (Axelsen, et al. 2006; Solan and Lampe, 2014). Cx43 S297 was observed to become dephosphorylated after 30 min of no-flow ischemia in Langendorff-perfused rat hearts whereas pretreatment with 10 nM rotigaptide could preserve the pS297 after 30 min of ischemia (Axelsen, et al. 2006). Additionally, cellular stress activates c-Jun N-terminal kinase (JNK), which is known to downregulate myocardial Cx43 expression, gap junction structure, and function under pathophysiological conditions (Petrich, et al. 2002). cAMP is known to exert a cardio-protective effect by PKA- and Epac-dependent signaling pathways that inhibit the stress-

activated JNK signaling pathway (Chae, et al. 2004; Kwak, et al. 2008; Sassone-Corsi, 2012). In conclusion, it seems feasible that AAP10 and rotigaptide may act via cAMP-dependent signaling pathways that inhibit the stress-activated JNK pathway which negatively affects Cx43-mediated myocardial gap junction formation and communication.

Author Contribution

XM performed all the electrophysiological experiments and current measurements; the immunoblots for Cx43 phosphoserine analysis using phospho-specific Cx43 antibodies were developed and performed by PDL; the experimental design, line graphs, and manuscript preparation were performed by RDV; neonatal mouse ventricular myocyte primary cultures were prepared by XM or RDV.

Acknowledgments and Funding Information:

This work was supported by NIH R01 grant HL-042220, and a Research Collaboration Agreement between Wyeth Research and the SUNY Research Foundation to RDV.

Ethical Approval

All experimental protocols involving mice were reviewed and approved by the SUNY Upstate Medical University Institutional Animal Care and Use Committee (IACUC).

Informed Consent

Not applicable

Competing Interests

The authors have no conflicts of interest to declare.

References

Ai X, Yan J, Pogwizd SM (2021) Serine-threonine protein phosphatase regulation of Cx43 dephosphorylation in arrhythmogenic disorders. Cell Signal 86:110070.

Aonuma S, Kohama Y, Makino T, Fujisawa Y (1982) Studies of heart. XXI. Amino acid sequence of antiarrhythmic peptide (AAP) isolated from atria. J Pharmacobiodyn 5:40-48.

Argentieri T, Cantor E, Wiggins JR (1989) Antiarrhythmic peptide has no direct cardiac actions. Experientia 45:737-738.

Atkinson MM, Lampe PD, Lin HH, Kollander R, Li XR, Kiang DT. (1995) Cyclic AMP modifies the cellular distribution of connexin43 and induces a persistent increase in the junctional permeability of mouse mammary tumor cells. J Cell Sci 108:3079-3090.

Axelsen LN, Stahlhut M, Mohammed S, Larsen BD, Nielsen MS, Holstein-Rathlou NH, Andersen S, Jensen ON, Hennan JK, Kjølbye AL (2006) Identification of ischemia-regulated phosphorylation sites in connexin43: A possible target for the antiarrhythmic peptide analogue rotigaptide (ZP123). J Mol Cell Cardiol 40:790-798.

Beardslee MA, Lerner DL, Tadros PN, Laing JG, Beyer EC, Yamada KA, Kléber AG, Schuessler RB, Saffitz JE (2000) Dephosphorylation and intracellular redistribution of ventricular connexin43 during electrical uncoupling induced by ischemia. Circ Res 87:656-662.

Bowling N, Huang X, Sandusky GE, Fouts RL, Mintze K, Esterman M, Allen PD, Maddi R, McCall E, Vlahos CJ (2001) Protein kinase C-alpha and -epsilon modulate connexin-43 phosphorylation in human heart. J Mol Cell Cardiol 33:789-798.

Burt JM, Spray DC (1988) Inotropic agents modulate gap junctional conductance between cardiac myocytes. Am J Physiol. 1988 254:H1206-H1210.

Chae HJ, Chae SW, Kim HR. (2004) Cyclic adenosine monophosphate inhibits nitric oxide-induced apoptosis of cardiac muscle cells in a c-Jun N-terminal kinase-dependent manner. Immunopharmacol Immunotoxicol 26:249-263.

Changri L, Sun H, Bao Y, Zhang M (2025) Rotigaptide inhibits spontaneous contractions of gastric smooth muscle in diabetic rats via the PKCα-Cx43 pathway. Cell Biol Int 49:92-100.

Clarke TC, Thomas D, Petersen JS, Evans WH, Martin PE (2006) The antiarrhythmic peptide rotigaptide (ZP123) increases gap junction intercellular communication in cardiac myocytes and HeLa cells expressing connexin 43. Br J Pharmacol 147:486-495.

Cooper CD, Lampe PD (2002) Casein kinase 1 regulates connexin-43 gap junction assembly. J Biol Chem 277:44962-44968.

Darrow BJ, Fast VG, Kléber AG, Beyer EC, Saffitz JE (1996) Functional and structural assessment of intercellular communication. Increased conduction velocity and enhanced connexin expression in dibutyryl cAMP-treated cultured cardiac myocytes. Circ Res 79:174-183.

Davis LM, Rodefeld ME, Green K, Beyer EC, Saffitz JE (1995) Gap junction protein phenotypes of the human heart and conduction system. J Cardiovasc Electrophysiol 6:813-822.

De Mello WC (1986) Interaction of cyclic AMP and Ca2+ in the control of electrical coupling in heart fibers. Biochim Biophys Acta 888:91-99.

De Mello WC (1989) Effect of isoproterenol and 3-isobutyl-1-methylxanthine on junctional conductance in heart cell pairs. Biochim Biophys Acta 1012:291-298.

De Mello WC, van Loon P (1987) Further studies on the influence of cyclic nucleotides on junctional permeability in heart. J Mol Cell Cardiol 19:763-771.

Dhein S, Hagen A, Jozwiak J, Dietze A, Garbade J, Barten M, Kostelka M, Mohr FW (2010) Improving cardiac gap junction communication as a new antiarrhythmic mechanism: the action of antiarrhythmic peptides. Naunyn Schmiedebergs Arch Pharmacol 381:221-234.

Dhein S, Larsen BD, Petersen JS, Mohr FW (2003) Effects of the new antiarrhythmic peptide ZP123 on epicardial activation and repolarization pattern. Cell Commun Adhes 10:371-378.

Dhein S, Manicone N, Müller A, Gerwin R, Ziskoven U, Irankhahi A, Minke C, Klaus W (1994) A new synthetic antiarrhythmic peptide reduces dispersion of epicardial activation recovery interval and diminishes alterations of epicardial activation patterns induced by regional ischemia. A mapping study. Naunyn Schmiedebergs Arch Pharmacol. 350:174-184.

Dhein S, Weng S, Grover R, Tudyka T, Gottwald M, Schaefer T, Polontchouk L (2001) Protein kinase Calpha mediates the effect of antiarrhythmic peptide on gap junction conductance. Cell Commun Adhes 8:257-264.

Doble BW, Ping P, Kardami E (2000) The epsilon subtype of protein kinase C is required for cardiomyocyte connexin-43 phosphorylation. Circ Res 86:293-301.

Doble BW, Dang X, Ping P, Fandrich RR, Nickel BE, Jin Y, Cattini PA, Kardami E (2004) Phosphorylation of serine 262 in the gap junction protein connexin-43 regulates DNA synthesis in cell-cell contact forming cardiomyocytes. J Cell Sci 117:507-514.

Dunn CA, Lampe PD (2014) Injury-triggered Akt phosphorylation of Cx43: a ZO-1-driven molecular switch that regulates gap junction size. J Cell Sci 127:455-464.

Ek-Vitorin JF, King TJ, Heyman NS, Lampe PD, Burt JM (2006) Selectivity of connexin 43 channels is regulated through protein kinase C-dependent phosphorylation. Circ Res 98:1498-1505.

Enomoto T, Yamasaki H (1985) Phorbol ester-mediated inhibition of intercellular communication in BALB/c 3T3 cells: relationship to enhancement of cell transformation. Cancer Res 45:2681-2688.

Hagen A, Dietze A, Dhein S (2009) Human cardiac gap-junction coupling: effects of antiarrhythmic peptide AAP10. Cardiovasc Res 83:405-415.

Haugan K, Marcussen N, Kjølbye AL, Nielsen MS, Hennan JK, Petersen JS (2006) Treatment with the gap junction modifier rotigaptide (ZP123) reduces infarct size in rats with chronic myocardial infarction. J Cardiovasc Pharmacol 2006 47:236-242.

Haugen K, Olsen KB, Hartvig L, Petersen JS, Holstein-Rathlou NH, Hennan JK, and Nielsen MS (2005) The antiarrhythmic peptide analog ZP123 prevents atrial conduction slowing during metabolic stress. J Cardiovasc Electrophysiol 16: 537-545.

Hennan JK, Swillo RE, Morgan GA, Keith JC Jr, Schaub RG, Smith RP, Feldman HS, Haugan K, Kantrowitz J, Wang PJ, Abu-Qare A, Butera J, Larsen BD, Crandall DL (2006) Rotigaptide (ZP123) prevents spontaneous ventricular arrhythmias and reduces infarct size during myocardial ischemia/reperfusion injury in open-chest dogs. J Pharmacol Exp Ther 317:236-243.

Hossain MZ, Ao P, Boynton AL (1998) Platelet-derived growth factor-induced disruption of gap junctional communication and phosphorylation of connexin43 involves protein kinase C and mitogen-activated protein kinase. J Cell Physiol 176:332-341.

Hossain MZ, Jagdale AB, Ao P, Boynton AL (1999) Mitogen-activated protein kinase and phosphorylation of connexin43 are not sufficient for the disruption of gap junctional communication by platelet-derived growth factor and tetradecanoylphorbol acetate. J Cell Physiol 179:87-96.

Kanemitsu MY, Jiang W, Eckhart W (1998) Cdc2-mediated phosphorylation of the gap junction protein, connexin43, during mitosis. Cell Growth Differ 9:13-21.

Kjølbye AL, Dikshteyn M, Eloff BC, Deschênes I, Rosenbaum DS (2008) Maintenance of intercellular coupling by the antiarrhythmic peptide rotigaptide suppresses arrhythmogenic discordant alternans. Am J Physiol Heart Circ Physiol 294:H41-H49.

Kjølbye AL, Knudsen CB, Jepsen T, Larsen BD, Petersen JS (2003) Pharmacological characterization of the new stable antiarrhythmic peptide analog Ac-D-Tyr-D-Pro-D-Hyp-Gly-D-Ala-Gly-NH2 (ZP123): in vivo and in vitro studies. J Pharmacol Exp Ther 306:1191-1199.

Koo SK, Kim DY, Park SD, Kang KW, Joe CO (1997) PKC phosphorylation disrupts gap junctional communication at G0/S phase in clone 9 cells. Mol Cell Biochem 167:41-49.

Kwak HJ, Park KM, Choi HE, Chung KS, Lim HJ, Park HY (2008) PDE4 inhibitor, roflumilast protects cardiomyocytes against NO-induced apoptosis via activation of PKA and Epac dual pathways. Cell Signal 20:803-814.

Lampe PD, Cooper CD, King TJ, Burt JM (2006) Analysis of connexin43 phosphorylated at S325, S328, S330 in normoxic and ischemic heart. J Cell Sci 119: 3435-3442.

Lampe PD, Kurata WE, Warn-Cramer B, Lau AP (1998) Formation of a distinct connexin43 phosphoisoform in mitotic cells is dependent upon p34cdc2 kinase. J Cell Sci 111: 833-841.

Lampe PD, TenBroek EM, Burt JM, Kurata WE, Johnson RG, Lau AF (2000) Phosphorylation of connexin43 on serine368 by protein kinase C regulates gap junctional communication. J Cell Biol 149:1503-1512.

Lin X, Gemel J, Beyer EC, Veenstra RD (2005) Dynamic model for ventricular junctional conductance during the cardiac action potential. Am J Physiol Heart Circ Physiol 288:H1113-1123.

Lin R, Warn-Cramer BJ, Kurata WE, Lau AF (2001) v-Src phosphorylation of connexin 43 on Tyr247 and Tyr265 disrupts gap junctional communication. J Cell Biol 154:815-827.

Lin X, Zemlin C, Hennan, JK, Petersen JS, Veenstra RD (2008) Enhancement of ventricular gap junction coupling by rotigaptide. Cardiovasc Res 79: 416-426.

Müller A, Gottwald M, Tudyka T, Linke W, Klaus W, Dhein S (1997) Increase in gap junction conductance by an antiarrhythmic peptide. Eur J Pharmacol 327:65-72.

Musil LS, Cunningham BA, Edelman GM, Goodenough DA (1990) Differential phosphorylation of the gap junction protein connexin43 in junctional communication-competent and -deficient cell lines. J Cell Biol 111:2077-2088.

Ni M, Ruan L, Zhang C (2015) Antiarrhythmic peptide AAP10 prevents arrhythmias induced by protein kinase C activation in rabbit left ventricular wedges. Int Heart J 56:234-238.

Park DJ, Wallick CJ, Martyn KD, Lau AF, Jin C, Warn-Cramer BJ (2007) Akt phosphorylates Connexin43 on Ser373, a "mode-1" binding site for 14-3-3. Cell Commun Adhes 14:211-226.

Petrich BG, Gong X, Lerner DL, Wang X, Brown JH, Saffitz JE, Wang Y (2002) c-Jun N-terminal kinase activation mediates downregulation of connexin43 in cardiomyocytes. Circ Res 91:640-647.

Sassone-Corsi P (2012) The cyclic AMP pathway. Cold Spring Harb Perspect Biol 4:a011148.

Shiroshita-Takeshita A, Sakabe M, Haugan K, Hennan JK, Nattel S (2007) Model-dependent effects of the gap junction conduction-enhancing antiarrhythmic peptide rotigaptide (ZP123) on experimental atrial fibrillation in dogs. Circulation 115:310-318.

Simon AM, Goodenough DA, Paul DL (1998) Mice lacking connexin40 have cardiac conduction abnormalities characteristic of atrioventricular block and bundle branch block. Curr Biol 8: 295-298.

Sirnes S, Kjenseth A, Leithe E, Rivedal E (2009) Interplay between PKC and the MAP kinase pathway in Connexin43 phosphorylation and inhibition of gap junction intercellular communication. Biochem Biophys Res Commun 382:41-45.

Solan JL, Lampe PD (2005) Connexin phosphorylation as a regulatory event linked to gap junction channel assembly. Biochim Biophys Acta 1711:154-163.

Solan JL, Lampe PD (2014) Specific Cx43 phosphorylation events regulate gap junction turnover in vivo. FEBS Lett 588:1423-1429.

Solan JL, Lampe PD (2020) Src Regulation of Cx43 Phosphorylation and Gap Junction Turnover. Biomolecules 10:1596.

Solan JL, Marquez-Rosado L, Sorgen PL, Thornton PJ, Gafken PR, Lampe PD (2007) Phosphorylation at S365 is a gatekeeper event that changes the structure of Cx43 and prevents down-regulation by PKC. J Cell Biol 179:1301-1309.

Somekawa S, Fukuhara S, Nakaoka Y, Fujita H, Saito Y, Mochizuki N (2005) Enhanced functional gap junction neoformation by protein kinase A-dependent and Epac-dependent signals downstream of cAMP in cardiac myocytes. Circ Res 97:655-662.

Stahlhut M, Petersen JS, Hennan JK, Ramirez MT (2006) The antiarrhythmic peptide rotigaptide (ZP123) increases connexin 43 protein expression in neonatal rat ventricular cardiomyocytes. Cell Commun Adhes 13:21-27.

Swenson KI, Piwnica-Worms H, McNamee H, Paul DL (1990) Tyrosine phosphorylation of the gap junction protein connexin43 is required for the pp60v-src-induced inhibition of communication. Cell Regul 1:989-1002.

Takemoto Y, Takanari H, Honjo H, Ueda N, Harada M, Kato S, Yamazaki M, Sakuma I, Opthof T, Kodama I, Kamiya K (2012) Inhibition of intercellular coupling stabilizes spiral-wave reentry, whereas enhancement of the coupling destabilizes the reentry in favor of early termination. Am J Physiol Heart Circ Physiol 303:H578-H586.

TenBroek EM, Lampe PD, Solan JL, Reynhout JK, Johnson RG (2001) Ser364 of connexin43 and the upregulation of gap junction assembly by cAMP. J Cell Biol 155:1307-1318.

Veenstra RD (2001) Voltage clamp limitations of dual whole-cell gap junction current and voltage recordings. I. Conductance measurements. Biophys J 80:2231-2247.

Warn-Cramer BJ, Lampe PD, Kurata WE, Kanemitsu MY, Loo LW, Eckhart W, Lau AF (1996) Characterization of the mitogen-activated protein kinase phosphorylation sites on the connexin-43 gap junction protein. J Biol Chem 271:3779-3786.

Wei S, Cassara C, Lin X, Veenstra RD (2019) Calcium-calmodulin gating of a pH-insensitive isoform of connexin43 gap junctions. Biochem J 476:1137-1148.

Weng S, Lauven M, Schaefer T, Polontchouk L, Grover R, Dhein S (2002) Pharmacological modification of gap junction coupling by an antiarrhythmic peptide via protein kinase C activation. FASEB J 16:1114-1116.

Xing D, Kjølbye AL, Nielsen MS, Petersen JS, Harlow KW, Holstein-Rathlou NH, and Martins JB (2003) ZP123 increases gap junctional conductance and prevents reentrant ventricular tachycardia during myocardial ischemia in open chest dogs. J Cardiovasc Electrophysiol 14: 510-520.